Article

Not All G-Quadruplexes Exhibit Ion-Channel-like Properties: NMR Study of Ammonium Ion (Non)movement within the d(GTG) Quadruplex

Primo ket, and Janez Plavec

J. Am. Chem. Soc., **2007**, 129 (28), 8794-8800• DOI: 10.1021/ja0710003 • Publication Date (Web): 20 June 2007

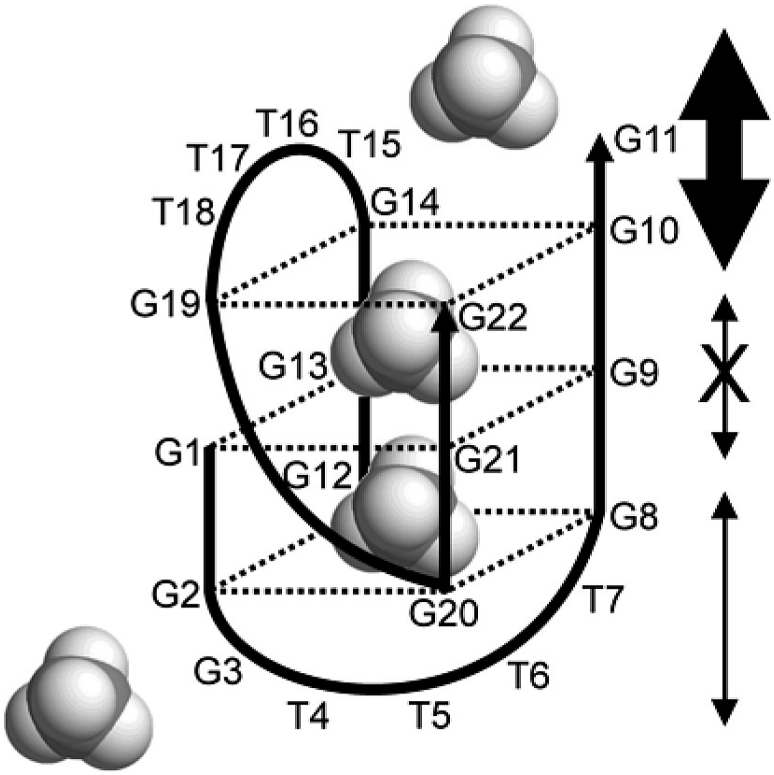

More About This Article

Additional resources and features associated with this article are available within the HTML version:

- Supporting Information
- Links to the 3 articles that cite this article, as of the time of this article download
- Access to high resolution figures
- Links to articles and content related to this article
- Copyright permission to reproduce figures and/or text from this article

J|A|C|S
ARTICLES
Published on Web 06/20/2007

Not All G-Quadruplexes Exhibit Ion-Channel-like Properties: NMR Study of Ammonium Ion (Non)movement within the $d(G_3T_4G_4)_2$ Quadruplex

Primož Šket and Janez Plavec*

Contribution from the Slovenian NMR Center, National Institute of Chemistry, Hajdrihova 19, SI-1000 Ljubljana, Slovenia

Received February 12, 2007; E-mail: janez.plavec@ki.si

Abstract: A solution-state NMR study on $^{15}NH_4^+$ ion movement within $d(G_3T_4G_4)_2$, a dimeric G-quadruplex consisting of three G-quartets and two T_4 loops, rather unexpectedly demonstrated the absence of $^{15}NH_4^+$ ion movement between the binding sites U and L along the central axis of the G-quadruplex. Distinct temperature dependences of autocorrelation signals for U and L binding sites have been observed in $^{15}N-^1H$ NzExHSQC spectra which correlate with the local stiffness of the G-quadruplex. The volumes of the cross-peaks, which are the result of $^{15}NH_4^+$ ion movement, have been interpreted in terms of rate constants, T_1 relaxation, and proton exchange. $^{15}NH_4^+$ ion movements from the binding sites U and L into the bulk solution are characterized by lifetimes of 139 ms and 1.7 s at 298 K, respectively. The 12 times faster movement from the binding site U demonstrates that $^{15}NH_4^+$ ion movement is controlled by the structure of T_4 loop residues, which through diagonal- vs edge-type orientations impose distinct steric restraints for cations to leave or enter the G-quadruplex. Arrhenius-type analysis has afforded an activation energy of 66 kJ mol^{-1} for the UB process, while it could not be determined for the LB process due to slow rates at temperatures below 298 K. We further the use of the $^{15}NH_4^+$ ion as an NMR probe to gain insight into the occupancy of binding sites by cations and kinetics of ion movement which are intrinsically correlated with the structural details, dynamic fluctuations, and local flexibility of the DNA structure.

Introduction

G-rich nucleic acid sequences, which are abundant throughout the genomes of many organisms, can form G-quadruplex structures.[1−7] Their involvement in various important biological functions has made G-quadruplexes important drug targets.[8,9] The main building blocks of G-quadruplex structures are stacks of square-planar arrays of G-quartets. A G-quartet consists of four guanines that are linked together by eight hydrogen bonds (Figure 1a). The presence of cations seems to be a prerequisite for G-quartet formation due to their role in reducing repulsions among guanine carbonyl oxygen atoms and additionally enhancing base-stacking interactions.[10,11] In general, cations can be localized along the central cavity of the G-quadruplex formed by the G-quartets, which are stacked in a regular geometry. However, cation coordination is not limited to a particular geometry within the G-quadruplex. A potential cation coordination site with four carbonyl oxygen atoms is in the plane of a G-quartet. Alternatively, cations can coordinate with eight carbonyl oxygen atoms between two stacked G-quartets. Considerable efforts using NMR[12−24] and X-ray crystallography[25−29]

(1) For a recent review see: Neidle, S.; Balasubramanian, S. *Quadruplex Nucleic Acids*; The Royal Society of Chemistry: Cambridge, U.K., 2006; p 301.
(2) Keniry, M. A. *Biopolymers* **2001**, *56*, 123−146.
(3) Davis, J. T. *Angew. Chem., Int. Ed.* **2004**, *43*, 668−698.
(4) Huppert, J. L.; Balasubramanian, S. *Nucleic Acids Res.* **2005**, *33*, 2908−2916.
(5) Todd, A. K.; Johnston, M.; Neidle, S. *Nucleic Acids Res.* **2005**, *33*, 2901−2907.
(6) Burge, S.; Parkinson, G. N.; Hazel, P.; Todd, A. K.; Neidle, S. *Nucleic Acids Res.* **2006**, *34*, 5402−5415.
(7) Phan, A. T.; Kuryavyi, V.; Patel, D. J. *Curr. Opin. Struct. Biol.* **2006**, *16*, 288−298.
(8) Sun, D. Y.; Thompson, B.; Cathers, B. E.; Salazar, M.; Kerwin, S. M.; Trent, J. O.; Jenkins, T. C.; Neidle, S.; Hurley, L. H. *J. Med. Chem.* **1997**, *40*, 2113−2116.
(9) Neidle, S.; Read, M. A. *Biopolymers* **2001**, *56*, 195−208.
(10) Hardin, C. C.; Perry, A. G.; White, K. *Biopolymers* **2001**, *56*, 147−194.
(11) Hud, N. V.; Plavec, J. The Role of Cations in Determining Quadruplex Structure and Stability in Quadruplex Nucleic Acids. In *Quadruplex Nucleic Acids*; Neidle, S., Balasubramanian, S., Eds.; The Royal Society of Chemistry: Cambridge, U.K., 2006; pp 100−130.
(12) Schultze, P.; Hud, N. V.; Smith, F. W.; Feigon, J. *Nucleic Acids Res.* **1999**, *27*, 3018−3028.
(13) Rovnyak, D.; Baldus, M.; Wu, G.; Hud, N. V.; Feigon, J.; Griffin, R. G. *J. Am. Chem. Soc.* **2000**, *122*, 11423−11429.
(14) Basu, S.; Szewczak, A.; Cocco, M.; Strobel, S. A. *J. Am. Chem. Soc.* **2000**, *122*, 3240−3241.
(15) Wu, G.; Wong, A. *Chem. Commun.* **2001**, 2658−2659.
(16) Crnugelj, M.; Hud, N. V.; Plavec, J. *J. Mol. Biol.* **2002**, *320*, 911−924.
(17) Wu, G.; Wong, A.; Gan, Z. H.; Davis, J. T. *J. Am. Chem. Soc.* **2003**, *125*, 7182−7183.
(18) Wong, A.; Wu, G. *J. Am. Chem. Soc.* **2003**, *125*, 13895−13905.
(19) Wong, A.; Ida, R.; Wu, G. *Biochem. Biophys. Res. Commun.* **2005**, *337*, 363−366.
(20) Ida, R.; Wu, G. *Chem. Commun.* **2005**, 4294−4296.
(21) Wu, G.; Wong, A. *Biochem. Biophys. Res. Commun.* **2004**, *323*, 1139−1144.
(22) Gill, M. L.; Strobel, S. A.; Loria, J. P. *J. Am. Chem. Soc.* **2005**, *127*, 16723−16732.
(23) Cevec, M.; Plavec, J. *Biochemistry* **2005**, *44*, 15238−15246.
(24) Ma, L.; Lezzi, M.; Kaucher, M. S.; Lam, Y. F.; Davis, J. T. *J. Am. Chem. Soc.* **2006**, *128*, 15269−15277.
(25) Laughlan, G.; Murchie, A. I. H.; Norman, D. G.; Moore, M. H.; Moody, P. C. E.; Lilley, D. M. J.; Luisi, B. *Science* **1994**, *265*, 520−524.
(26) Phillips, K.; Dauter, Z.; Murchie, A. I. H.; Lilley, D. M. J.; Luisi, B. *J. Mol. Biol.* **1997**, *273*, 171−182.
(27) Horvath, M. P.; Schultz, S. C. *J. Mol. Biol.* **2001**, *310*, 367−377.
(28) Haider, S.; Parkinson, G. N.; Neidle, S. *J. Mol. Biol.* **2002**, *320*, 189−200.

10.1021/ja0710003 CCC: $37.00

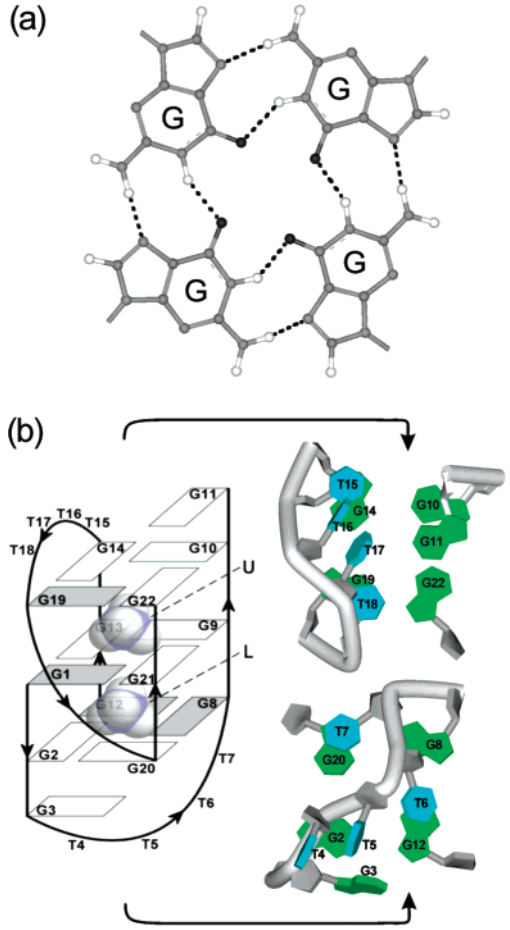

Figure 1. (a) G-quartet. (b) Folding topology with the location of ammonium ions within the dimeric fold-back structure adopted by $d(G_3T_4G_4)_2$. G1−G11 and G12−G22 indicate residues in the two strands. The guanine bases are shown as rectangles, where filled gray rectangles represent *syn* nucleobases. Thymine bases are omitted for clarity. Labels U and L indicate ammonium ions at the two different binding sites. Bird's-eye view of the 3D structure (PDB id 1U64) with the diagonal loop consisting of G3−T7 residues (bottom right) and the edge-type loop consisting of T15−T18 residues (top right).

have been made to localize monovalent cations such as K^+, Rb^+, and Tl^+ between pairs of adjacent G-quartets. On the other hand, Na^+ ions have demonstrated their ability to coordinate both between and within G-quartet planes presumably due to their smaller ionic radii. Recently, Hud and Feigon et al. have utilized ^{15}N-labeled ammonium ions as a nonmetallic probe and showed that three $^{15}NH_4^+$ ions are localized between each stacked pair of four G-quartet planes within $d(G_4T_4G_4)_2$, a dimeric G-quadruplex comprising four G-quartets with T_4 loops spanning across diagonals of the outer G-quartets.[30,31] An X-ray crystallographic study on the same G-quadruplex has shown five bound K^+ ions, with two of them between the outer G-quartet and loop residues.[28] No $^{15}NH_4^+$ ion binding sites could be detected by NMR that involved thymine loops, indicating either that $^{15}NH_4^+$ ions do not coordinate in the loops in solution or that the relative affinity in the loops is lower than between the G-quartets and/or their exchange is fast on the NMR time scale and therefore no resolved signal can be observed.[31−34] In general, G-quadruplexes are stabilized by monovalent cations in the following order: $K^+ > {}^{15}NH_4^+ > Na^+ > Rb^+ > Cs^+ \gg Li^+$.[12,35,36] It has been shown that the preferential binding of K^+ versus Na^+ to the $d(G_3T_4G_3)_2$ G-quadruplex is not dominated by a better fit of K^+ ions into the cavity between the two G-quartet planes, but rather by the smaller free energy of dehydration for K^+ in comparison to Na^+ ions.[37] Cations within G-quadruplex structures are not bound statically,[31,36] which has stimulated explorations of G-quadruplexes as synthetic transmembrane ion channels.[3,38] Data on cation mobility are however scarce, which warrants further studies into the understanding and control of cation mobility within the G-quadruplex and DNA in general.

We have recently described NMR assignment and 3D structure determination of the $d(G_3T_4G_4)_2$ G-quadruplex as well as explored its two cation binding sites.[39−41] $d(G_3T_4G_4)_2$ adopts a dimeric G-quadruplex structure with three G-quartets, two loops that span across the diagonal and edge of the outer G-quartets, and the unusual chain reversal that is not mediated by a nucleotide residue (Figure 1b). The structure is composed of three parallel strands and one antiparallel strand. Interestingly, this type of (3 + 1) topology has been described recently for sequences containing four units of human telomer repeat in the presence of K^+ ions.[42−44] $d(G_3T_4G_4)_2$ exhibits two cation binding sites, U and L, that differ in their preference for K^+, $^{15}NH_4^+$, and Na^+ ions, albeit the same structure is retained with a change of the cation.[40] In the present work we extend our exploration of cation interactions within the central cavities of G-quadruplexes by analyzing $^{15}NH_4^+$ ion movement within $d(G_3T_4G_4)_2$ and with the bulk solution. Somewhat surprisingly, we have noticed that $^{15}NH_4^+$ ions do not exchange between the two cation binding sites within $d(G_3T_4G_4)_2$. $^{15}NH_4^+$ ion movement within $d(G_3T_4G_4)_2$ is strikingly different from that of the closely related molecule $d(G_4T_4G_4)_2$ under similar conditions. Apart from the absence of $^{15}NH_4^+$ ion movement within $d(G_3T_4G_4)_2$, their movement to the bulk is slower from one of the two binding sites. Our findings give insight into how structural details of the G-quadruplex play a role in controlling cation transport and its kinetics along the central axis, which is of relevance for biological function and in assembly of nanodevices such as synthetic ion channels.

(29) Caceres, C.; Wright, G.; Gouyette, C.; Parkinson, G.; Subirana, J. A. *Nucleic Acids Res.* **2004**, *32*, 1097−1102.
(30) Hud, N. V.; Schultze, P.; Feigon, J. *J. Am. Chem. Soc.* **1998**, *120*, 6403−6404.
(31) Hud, N. V.; Schultze, P.; Sklenar, V.; Feigon, J. *J. Mol. Biol.* **1999**, *285*, 233−243.
(32) Sket, P.; Crnugelj, M.; Kozminski, W.; Plavec, J. *Org. Biomol. Chem.* **2004**, *2*, 1970−1973.
(33) Dingley, A. J.; Peterson, R. D.; Grzesiek, S.; Feigon, J. *J. Am. Chem. Soc.* **2005**, *127*, 14466−14472.
(34) Podbevsek, P.; Hud, N. V.; Plavec, J. *Nucleic Acids Res.* **2007**, *35*, 2554−2563.
(35) Guschlbauer, W.; Chantot, J. F.; Thiele, D. *J. Biomol. Struct. Dyn.* **1990**, *8*, 491−511.
(36) Deng, H.; Braunlin, W. H. *J. Mol. Biol.* **1996**, *255*, 476−483.
(37) Hud, N. V.; Smith, F. W.; Anet, F. A. L.; Feigon, J. *Biochemistry* **1996**, *35*, 15383−15390.
(38) Kaucher, M. S.; Harrell, W. A.; Davis, J. T. *J. Am. Chem. Soc.* **2006**, *128*, 38−39.
(39) Crnugelj, M.; Sket, P.; Plavec, J. *J. Am. Chem. Soc.* **2003**, *125*, 7866−7871.
(40) Sket, P.; Crnugelj, M.; Plavec, J. *Bioorg. Med. Chem.* **2004**, *12*, 5735−5744.
(41) Sket, P.; Crnugelj, M.; Plavec, J. *Nucleic Acids Res.* **2005**, *33*, 3691−3697.
(42) Luu, K. N.; Phan, A. T.; Kuryavyi, V.; Lacroix, L.; Patel, D. J. *J. Am. Chem. Soc.* **2006**, *128*, 9963−9970.
(43) Xu, Y.; Noguchi, Y.; Sugiyama, H. *Bioorg. Med. Chem.* **2006**, *14*, 5584−5591.
(44) Ambrus, A.; Chen, D.; Dai, J. X.; Bialis, T.; Jones, R. A.; Yang, D. Z. *Nucleic Acids Res.* **2006**, *34*, 2723−2735.

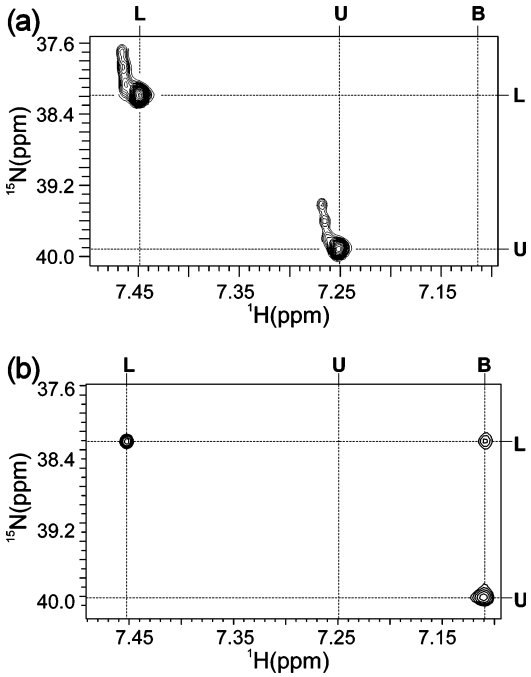

Figure 2. 2D ^{15}N−^{1}H NzExHSQC spectra of d($G_3T_4G_4$)$_2$ at 298 K and pH 4.5 in 10% $^{2}H_2O$ at mixing times of 13 ms (a) and 1.6 s (b). The positions of the signals and respective cross-peaks are labeled. The large autocorrelation peak of the bulk $^{15}NH_4^+$ ions (δ_{1H} = 7.11 ppm, δ_{15N} = 30 ppm) is outside the shown region. The oligonucleotide concentration was 3.0 mM in strand, while the concentration of $^{15}NH_4Cl$ was 50 mM.

Methods

Experimental Details. An NMR sample of oligonucleotide d($G_3T_4G_4$) was prepared as described previously.[39] The concentration was 3 mM in strand (1.5 mM in G-quadruplex) with a pH of 4.5 which was adjusted with LiOH or HCl. $^{15}NH_4Cl$ was titrated into the sample to 50 mM concentration. All NMR spectra were collected on a Varian Unity Inova 600 MHz NMR spectrometer in the 273−298 K temperature range. The mixing times of 2D ^{15}N−^{1}H NzExHSQC spectra were set between 13 ms and 10 s. If not stated otherwise, volume integrals were expressed relative to the autocorrelation peak U at a mixing time of 13 ms, which was assigned an arbitrary volume of 100 units. Iterative least-squares fitting was done with Origin 7.5 software (www.originlab.com).

Results

The d($G_3T_4G_4$)$_2$ G-Quadruplex Exhibits Two Cation Binding Sites. d($G_3T_4G_4$) has been folded into a G-quadruplex upon an increase of the $^{15}NH_4Cl$ concentration to 50 mM. The ^{1}H NMR spectrum has offered good spectral resolution in which signals corresponded to a single species in solution and enabled determination of the 3D structure.[39,40] Further NMR experiments helped us to establish two cation binding sites, U and L, within the dimeric d($G_3T_4G_4$)$_2$ G-quadruplex structure.[41] Both $^{15}NH_4^+$ ion binding sites are located between two adjacent G-quartets (Figure 1b), which are experimentally verified by the two autocorrelation peaks in ^{15}N−^{1}H NzExHSQC spectra (Figure 2a). In addition to the autocorrelation peaks, we expected to observe cross-peaks corresponding to the movement of $^{15}NH_4^+$ ions between different binding sites.

Apparent $^{15}NH_4^+$ Ion Occupancy of L and U Binding Sites within d($G_3T_4G_4$)$_2$. In the course of titration of an aqueous solution of d($G_3T_4G_4$) with $^{15}NH_4^+$ ions, the volume integrals for cross-peaks in standard 2D ^{15}N−^{1}H HSQC spectra corresponding to U and L binding sites reached a plateau at 8 mM concentration (i.e., 5.3 equiv with respect to the G-quadruplex). Nevertheless, even at the 50 mM $^{15}NH_4^+$ ion concentration used in the current study, the autocorrelation peak volumes corresponding to U and L binding sites were not equal as would be expected for the two binding sites with equal occupancy. The volume ratio of the autocorrelation peaks corresponding to U and L binding sites (V_U/V_L ratio) was 0.8 at 298 K. The smaller apparent occupancy of binding site U at 298 K has been attributed to the faster movement of $^{15}NH_4^+$ ions from this site (vide infra). The variation of the V_U/V_L ratio as a function of temperature can be described by a linear relationship (Figure S1 in the Supporting Information). The V_U/V_L ratio increases from 0.8 at 298 K to 1.3 at 278 K. The movement of $^{15}NH_4^+$ ions from binding site U becomes slower at lower temperature, while it is much slower from binding site L already at 298 K. The data point at 273 K is not on the straight line, which suggests that the V_U/V_L ratio has reached a plateau (Figure S1). It should be noted, however, that volume integrals of autocorrelation peaks in HSQC spectra depend in a more complicated way on the amount of $^{15}NH_4^+$ ions localized at a given binding site and the rate of $^{15}NH_4^+$ ion movement as well as on other factors including relaxation and proton exchange, which are binding site dependent.

Unique Regime of $^{15}NH_4^+$ Ion Movement. A series of 2D ^{15}N−^{1}H NzExHSQC experiments with mixing times in the range from 13 ms to 10 s have been recorded at 298 K. The observation of the autocorrelation and cross-peaks at mixing times as long as 10 s has suggested slow T_1 relaxation. Nevertheless, no cross-peaks corresponding to $^{15}NH_4^+$ ion movement between binding sites U and L have been observed, which is a novel observation on cation (non)movement within a G-quadruplex structure (Figure 2). In contrast, two cross-peaks, UB and LB, clearly demonstrate that $^{15}NH_4^+$ ions move from binding sites U and L into the bulk solution (Figure 2b). The signal intensities of autocorrelation peaks U, L, and B decrease, while the intensities of UB and LB cross-peaks increase with increasing mixing time of the NzExHSQC experiment (Figure 2). Distinct intensities of UB and LB cross-peaks as a function of the mixing time (τ_m) have shown that movement from binding site U into the bulk is by far more effective than the movement from binding site L. While autocorrelation peak U disappears at a mixing time of ∼700 ms, the peak for L can be observed till a mixing time of 3 s.

Decrease of Autocorrelation peaks U, L, and B. The intensity of autocorrelation peaks U and L is expected to decrease as a function of the mixing time (τ_m) due to $^{15}NH_4^+$ ion movement from the original position at the binding site within d($G_3T_4G_4$)$_2$ to the bulk solution as well as due to relaxation (T_{1a}) which can be described by eq 1 where V_a

$$V_a(\tau_m) = A[e^{-B\tau_m}] = A[e^{-[k_N+(1/T_{1a})]\tau_m}] \qquad (1)$$

represents the volume integral of an autocorrelation peak, A is the scaling factor, B is the rate constant, and τ_m is the mixing time used in the 2D NzExHSQC experiment. As suggested by the right-hand side of eq 1, the rate constant B can be dissected into the sum of the rate constant for $^{15}NH_4^+$ ion movement (k_N) and the reciprocal value of the spin−lattice relaxation time for the autocorrelation peak (T_{1a}). Our initial fits demonstrated, however, that the experimental decrease of autocorrelation peaks

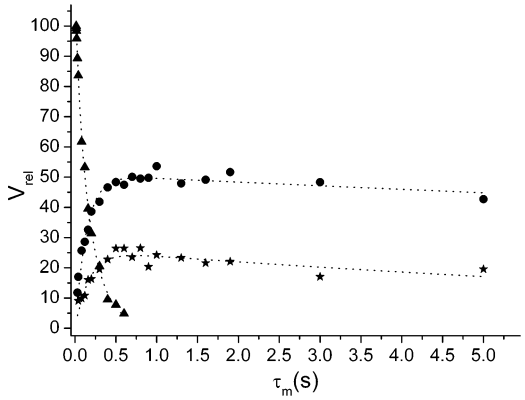

Figure 3. Relative volumes of autocorrelation peak U (triangles) and cross-peaks UB (circles) and BU (stars) as a function of the mixing time (τ_m) at 298 K. Dotted curves represent the best fits of the experimental data points to eqs 2 and 3. The parameters that best fit the volume integrals of U are $A_1 = 23 \pm 12$, $B_1 = 19 \pm 11$ s^{-1}, $A_2 = 88 \pm 14$, and $B_2 = 5.1 \pm 0.5$ s^{-1} with individual deviations below 3 and an rmsd of 1.3 arbitrary volume units ($R = 0.999$). The least-squares fit of V_{UB} from 30 ms to 5 s is characterized by individual deviations below 5 and an rmsd of 2.1 arbitrary volume units ($R = 0.984$). The agreement between the experimental and calculated data points of V_{BU} is characterized by individual deviations below 4 and an rmsd of 2.0 arbitrary volume units ($R = 0.927$).

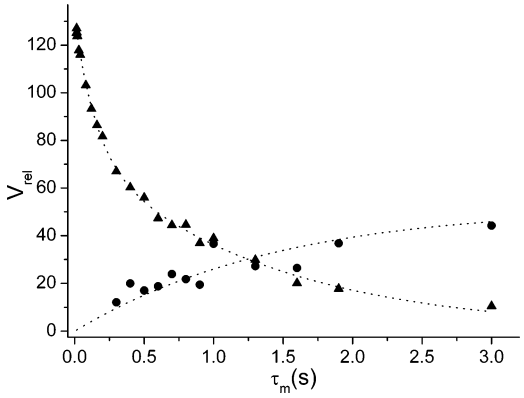

Figure 4. Relative volumes of autocorrelation peak L (triangles) and cross-peak LB (circles) as a function of the mixing time (τ_m) at 298 K. Dotted curves represent the best fits of the experimental data to eqs 2 and 3, respectively. The parameters that best fit the experimental data for L are $A_1 = 55 \pm 3$, $B_1 = 7 \pm 1$ s^{-1}, $A_2 = 76 \pm 3$, and $B_2 = 0.8 \pm 0.1$ s^{-1} with individual deviations below 3 and an rmsd of 1.6 arbitrary volume units ($R = 0.999$). The agreement between the experimental and calculated data points of V_{LB} using eq 3 is characterized with individual deviations below 11 and an rmsd of 5.1 arbitrary volume units ($R = 0.825$).

L, U, and B as a function of the mixing time could not be adequately accounted for by eq 1 using a single-exponential function. At shorter mixing times the decrease of the autocorrelation peak is steep, whereas at longer τ_m values the signal decrease is slower and does not converge to zero as expected from a single-exponential function. The volumes of the autocorrelation peaks can be better described by a biexponential function,[45] eq 2

$$V_a(\tau_m) = A_1[e^{-B_1\tau_m}] + A_2[e^{-B_2\tau_m}] \qquad (2)$$

where A_1 and A_2 are scaling factors and exponents B_1 and B_2 are rate constants. The best fit to the experimental data for autocorrelation peak U is shown in Figure 3.

As movement of $^{15}NH_4^+$ ions from binding site L to the bulk solution was slow, we expected that the intensity of autocorrelation peak L would decrease mainly due to longitudinal relaxation. However, the experimental data showed a biexponential decrease that was described better by eq 2 (Figure 4).

Due to a great excess of bulk $^{15}NH_4^+$ ions in comparison to the amount of ions bound within d($G_3T_4G_4$)$_2$, the decrease in intensity of autocorrelation peak B with the mixing time was expected to occur mainly due to relaxation and proton exchange with water.[46] The least-squares analysis of the volume integrals (V_B) as a function of the mixing time using a single exponent (eq 1) could not provide a satisfactory fit. A steep decrease of autocorrelation peak B was observed at mixing times (τ_m) up to 80 ms, which was followed by a moderate decrease at longer mixing times (Figure 5). At a mixing time of 10 s the volume integral of autocorrelation peak B was ca. 50% of the value at 13 ms. The shape of the function that fits the experimental data suggests a biexponential decrease described by eq 2 (Figure 5). Assuming that rate constant B_2 corresponds to relaxation gives a T_{1B} relaxation time of 31 s (i.e., $1/B_2$). It is noteworthy

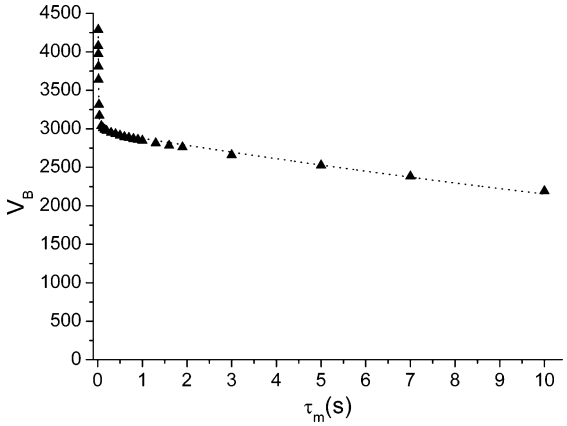

Figure 5. Volume of autocorrelation peak B as a function of the mixing time (τ_m) at 298 K. Triangles represent the experimental data points at 298 K, while the dotted curve represents the best fit to eq 2 with the following parameters: $A_1 = 3455 \pm 303$, $B_1 = 80 \pm 6$ s^{-1}, $A_2 = 2971 \pm 12$, and $B_2 = 0.032 \pm 0.002$ s^{-1}. The agreement between the experimental and calculated data points was good with individual deviations below 95 and an rmsd of 38 arbitrary volume units ($R = 0.997$).

that the same results for a decrease of autocorrelation peak B are observed in the absence of the G-quadruplex, i.e., when only $^{15}NH_4^+$ ions are present in solution.

The ammonium ion possesses four protons which are directly attached to the ^{15}N nucleus, and therefore, intramolecular dipolar interactions are expected to be the dominant mode of relaxation.[47] However, many other mechanisms can contribute to efficiency of relaxation. $^{15}NH_4^+$ ions are localized between two stacked G-quartets, and libration of guanine imino protons within G-quartets or dynamic motions, which operate on time scales different from that of inter- or intramolecular dipole−dipole relaxation, represent alternative relaxation pathways. Overall T_1 relaxation is a sum of various relaxation processes which are in addition influenced by cross-correlation effects. Interestingly, the presence of different amounts of deuterated water in the sample (0−50%) does not affect the overall shape of the volume

(45) Kay, L. E.; Nicholson, L. K.; Delaglio, F.; Bax, A.; Torchia, D. A. *J. Magn. Reson.* **1992**, *97*, 359−375.
(46) Kettani, A.; Gueron, M.; Leroy, J. L. *J. Am. Chem. Soc.* **1997**, *119*, 1108−1115.
(47) Wei, A.; Raymond, M. K.; Roberts, J. D. *J. Am. Chem. Soc.* **1997**, *119*, 2915−2920.

decrease of $^{15}NH_4^+$ ions in bulk solution as a function of the mixing time nor autocorrelation peak volumes at long mixing times.

U and L Autocorrelation Peaks Show a Distinct Temperature Dependence. A series of 2D $^{15}N-^{1}H$ NzExHSQC experiments with mixing times from 13 ms to 1.6 s in the temperature range from 273 to 298 K have been recorded in 5 K steps. The autocorrelation peak for binding site U shows considerable changes of its volume integral with temperature (Figure S2a in the Supporting Information). At all temperatures the steep slopes at shorter mixing times up to ~200−300 ms are followed by a more moderate decrease at longer mixing times. At 298 K the volume of autocorrelation peak U drops by 80% till a mixing time of 300 ms. On the other hand, it drops by only 40% till the same mixing time at 273 K. The decrease of autocorrelation peak U varies with temperature, which has to be correlated with the rate of $^{15}NH_4^+$ ion movement. The rate constants B_1 (6−19 s^{-1}) and B_2 (0.4−5.1 s^{-1}) that best fit the experimental volume integrals for binding site U as a function of the mixing time using eq 2 increase with an increase of temperature from 273 to 298 K (Table S1 in the Supporting Information).

Temperature variation of a decrease of volume of autocorrelation peak L as a function of the mixing time in the 273−298 K temperature range shows almost negligible variation with temperature (Figure S2b). The rate constant B_1 shows a slight decrease from 11 to 7 s^{-1}, while rate constant B_2 (0.8 s^{-1}) does not exhibit temperature dependence from 273 to 298 K (Table S1).

Exchange Rate Constants for $^{15}NH_4^+$ Ion Movement between Binding Site U and the Bulk. The UB cross-peak is expected to increase as a function of the mixing time (τ_m) as $^{15}NH_4^+$ ions move from binding site U into the bulk solution. At the same time the UB cross-peak decreases due to relaxation (T_{1UB}). In the simplest way, the volume integral of a cross-peak is defined by a combination of two effects which can be described by the following equation:

$$V_c(\tau_m) = Af[e^{-(\tau_m/T_{1c})}(1 - e^{-k_N\tau_m})] \quad (3)$$

where V_c represents the volume integral of a cross-peak (e.g., UB), T_{1c} is the corresponding spin−lattice relaxation time, τ_m is the mixing time of the 2D NzExHSQC experiment, and k_N corresponds to the rate constant for $^{15}NH_4^+$ ion movement (e.g., k_{UB}). Parameter A is a scaling factor and represents the sum of scaling factors A_1 and A_2 obtained through the analysis of the corresponding autocorrelation peak using eq 2. It was kept fixed during the iterative fitting. Parameter f represents reduction of V_c due to a loss in cross-peak volume by proton exchange. In the special case with no proton exchange between $^{15}NH_4^+$ ions in the bulk solution and surrounding water molecules, parameter f would be 1.

Analysis of the volume of UB cross-peak reveals that its maximum value is reached at a mixing time of ~700 ms (Figure 3). At the same mixing time the volume of autocorrelation peak U drops to zero. $^{15}NH_4^+$ ions which were located at binding site U at the beginning of the NMR experiment moved into the bulk solution or underwent T_1 relaxation. Volumes of the UB cross-peak could not be accurately determined at mixing times shorter than 30 ms due to their low intensity. The first part of the UB curve up to a mixing time of ~700 ms is related to an increase of the cross-peak's volume due to $^{15}NH_4^+$ ion movement defined by k_{UB}. At longer τ_m values the curvature is governed by T_1 relaxation (Figure 3). The corresponding rate constant k_{UB} is 7.2 ± 0.5 s^{-1} and factor f is 0.46 ± 0.01. The movement of $^{15}NH_4^+$ ions from binding site U into the bulk is therefore characterized by a residence time ($1/k_{UB}$) of approximately 139 ms at 298 K. The iterative fitting procedure showed that the best fit of the experimental data to eq 3 is not very sensitive to the T_{1UB} relaxation time. The slope of the curve is gentle after the maximum point has been reached, which is consistent with slow T_1 relaxation. The optimized value for T_{1UB} was 39 ± 18 s.

As the system is under equilibrium conditions, $^{15}NH_4^+$ ions are also moving in the reverse direction from the bulk to binding site U. The least-squares fit of the experimental data as a function of mixing time using eq 3 provided a rate constant k_{BU} of 5.8 ± 0.9 s^{-1}. Interestingly, the BU cross-peak is characterized by a smaller relaxation time (T_{1BU}) of 12 ± 4 s at 298 K (Figure 3). Relaxation of $^{15}NH_4^+$ ions inside the G-quadruplex is more effective than in the bulk solution.

Activation Energy for the Movement of $^{15}NH_4^+$ Ions from Binding site U into the Bulk Solution. The kinetic profiles of $^{15}NH_4^+$ ion movement from binding site U to the bulk were determined in the temperature range from 273 to 298 K in 5 K steps. The rate constant k_{UB} is reduced considerably at lower temperatures. At 273 and 278 K the UB cross-peak appeared only at mixing times longer than 900 ms. The volume integrals were very weak at temperatures below 283 K, which prevented their quantitative analysis. The use of an Arrhenius relation based on k_{UB} rate constants in the 283−298 K temperature range afforded an activation energy (E_a) of 66 ± 8 kJ mol^{-1} (Figure S3 in the Supporting Information). The corresponding activation enthalpy and entropy values according to Eyring theory are 63 kJ mol^{-1} and −17 J $mol^{-1}K^{-1}$, respectively.

$^{15}NH_4^+$ Ion Movement from Binding Site L into the Bulk. LB cross-peak volumes were used to determine the exchange rate constant k_{LB} using eq 3. The LB volume integrals increase to a mixing time (τ_m) of 3 s (Figure 4). At longer mixing times, the integration of the LB cross-peak was prevented due to t_1 noise along the chemical shift of autocorrelation peak B. The fact that autocorrelation peak L does not reach zero after 3 s is in agreement with slow movement of $^{15}NH_4^+$ ions to the bulk and slow T_1 relaxation. Relaxation time T_{1LB} is however poorly defined by the experimental data, and the value of 39 s obtained for cross-peak UB was used in the fitting procedure. As $^{15}NH_4^+$ ions that move from binding site L into bulk solution are probably exposed to the same proton exchange as ions that move from binding site U, a scaling factor f of 0.46 has been used in the fitting to eq 3. The least-squares fit of the volume integrals (V_{LB}) as a function of the mixing time in the range from 0.3 to 3 s at 298 K afforded a rate constant k_{LB} of 0.6 ± 0.1 s^{-1} (Figure 4). The residence time for the $^{15}NH_4^+$ ion occupying binding site L is thus ~1.7 s at 298 K. It is noteworthy that the volumes of the LB cross-peaks were small at temperatures below 298 K, which prevented quantitative analyses of the k_{LB} rate constants at lower temperatures and thus determination of the activation energy.

Discussion

The dimeric $d(G_3T_4G_4)_2$ G-quadruplex structure consists of three G-quartet planes with the two outer G-quartets spanned

by diagonal- and edge-type loops. It represents a good model system to evaluate how structural features can control hopping of cations along the central cavity and into the bulk solution. The structure of $d(G_3T_4G_4)_2$ exhibits two $^{15}NH_4^+$ ion binding sites, which have been labeled as U and L. Although both binding sites are localized between the two stacked G-quartets, they are different in their thermodynamic and kinetic properties, which is also reflected in a considerable difference in the proton as well as nitrogen chemical shifts of bound $^{15}NH_4^+$ ions. We have demonstrated previously that the two cation binding sites within the G-quadruplex core differ to such a degree that $^{15}NH_4^+$ ions at binding site U are replaced first during titration with K^+ ions.[41] Upon a further increase in the concentration of K^+ ions, both binding sites are taken up by K^+ ions. Interestingly, the three dication forms have been involved in slow exchange on the NMR time scale.[41] In the present investigation we extend our studies and focus on the dynamics of $^{15}NH_4^+$ ion movement within $d(G_3T_4G_4)_2$. Our experimental data unequivocally prove that $^{15}NH_4^+$ ions do not move between binding sites U and L. This observation is in contrast to $^{15}NH_4^+$ ion movement between the three binding sites inside the closely related $d(G_4T_4G_4)_2$ G-quadruplex, where $^{15}NH_4^+$ ions have been shown to move back and forth along the central cation cavity.[31] Additionally, autocorrelation and cross-peak signals for $d(G_3T_4G_4)_2$ are much longer lived and are observed till mixing times up to 5 s.

$^{15}NH_4^+$ ions move from binding sites U and L into the bulk solution. The comparison of volumes of UB and LB cross-peaks has demonstrated that movement of $^{15}NH_4^+$ ions from binding site U to the bulk solution is 12 times more frequent. The corresponding rate constants are 7.2 and 0.6 s^{-1} for the UB and LB processes at 298 K, respectively. The examination of the 3D structure along the central axis of $d(G_3T_4G_4)_2$ has revealed that the diagonal loop represents a larger steric hindrance for cations to leave the G-quadruplex core in comparison to the edge-type loop (Figure 1b). Nevertheless, steric restraints of the diagonal loop do not prevent $^{15}NH_4^+$ ion movement from binding site L into the bulk although it requires structural change. $^{15}NH_4^+$ ions at binding site L could hypothetically move to binding site U from where the ions are in faster exchange with the bulk solution. However, the energetic barrier for the movement between the two binding sites is evidently too high, indicating that partial opening of the middle G-quartet, which is required for ions to get through, is energetically a more demanding process than opening of the outer G-quartet followed by a conformational change of the diagonal loop. Moreover, in such a hypothetical case the G-quadruplex structure without $^{15}NH_4^+$ ions would be unstable and would probably unfold. The structure of the loops also controls the efficiency of $^{15}NH_4^+$ ion movement into the G-quadruplex. The rate constant k_{BU} of 5.8 s^{-1} corresponds to movement of $^{15}NH_4^+$ ions from the bulk to binding site U at 298 K. The comparison of the k_{UB} and k_{BU} rate constants could suggest that $^{15}NH_4^+$ ion movement from the bulk into the G-quadruplex is slower than the reverse process. The analysis of the individual rate constant is however complicated due to different relaxation times in the bulk and within the G-quadruplex as well as by imprecision of the integration of cross-peak BU in proximity of the huge autocorrelation signal of bulk $^{15}NH_4^+$ ions. As a result, the k_{UB} and k_{BU} rate constants are essentially the same within experimental error. The actual rate of $^{15}NH_4^+$ ion movement from the bulk solution into the G-quadruplex is probably influenced by the bulk $^{15}NH_4^+$ ion concentration in a complex way. The movement in the reversed direction is in addition influenced by the concentration of the G-quadruplex. In the simplest case of first-order kinetics the ratio of rate constants for $^{15}NH_4^+$ ion movement out of and into the $d(G_3T_4G_4)_2$ G-quadruplex can be used to estimate the equilibrium binding constant and respective populations of vacant and occupied binding sites. The population of vacant binding sites would be below a few percent, which clearly has to be considered as the upper limit. In complete agreement, there is no experimental evidence of vacant binding sites within the $d(G_3T_4G_4)_2$ G-quadruplex which are long-lived and result in a separate set of signals with distinct chemical shifts corresponding to a combination of partially occupied species.

It is interesting to note that in the course of titration of single-stranded $d(G_3T_4G_4)$ we have observed that the appearance of imino protons corresponding to the folded G-quadruplex is strictly correlated with the appearance of two bound $^{15}NH_4^+$ ion signals simultaneously. For example, at a 0.8 mM concentration of $^{15}NH_4^+$ ions (ca. 0.5 equiv with respect to the hypothetical G-quadruplex) the majority of oligonucleotide is present as a single strand (Figure S4 in the Supporting Information). It is impossible to prepare the $d(G_3T_4G_4)_2$ G-quadruplex structure with 50% occupancy of cation binding sites, where either binding site U or binding site L would be occupied by $^{15}NH_4^+$ ions. $^{15}NH_4^+$ ions at binding sites U and L which exhibit equal intensities are both important for G-quadruplex formation (Figure S4b). A further increase in the concentration of $^{15}NH_4^+$ ions leads to more folding of oligonucleotide $d(G_3T_4G_4)$ into the G-quadruplex structure (Figure S5 in the Supporting Information). In the course of titration single-stranded and G-quadruplex structures of $d(G_3T_4G_4)$ are in slow exchange on the NMR time scale.

$^{15}NH_4^+$ ions in the bulk solution are exposed to efficient proton exchange above pH 3.[46] This is demonstrated through broadening of autocorrelation peak B, which has served as an internal pH meter. The volumes of cross-peaks corresponding to the movement of $^{15}NH_4^+$ ions from binding sites U and L into the bulk also critically depend on the pH value of the sample. In the case of the UB and LB cross-peaks we have observed 54% loss of signal by proton exchange at pH 4.5 and 298 K. An increase of pH to 5.5 resulted in 70% loss of the cross-peak volumes at 298 K. Higher pH values result in broader spectral lines which complicate their quantitative analyses.

The decrease of the volume integrals of the autocorrelation peaks has been interpreted in terms of a biexponential function. A steep decrease of the volumes of autocorrelation peaks U and L at shorter mixing times ($\tau_m \approx 200-300$ ms at 298 K) is followed by a more moderate decrease at longer mixing times. The steepest decrease at short mixing times has been observed for autocorrelation peak B and interpreted in terms of very efficient proton exchange with water. The decrease of autocorrelation peaks U and L is not pH dependent, which suggests that proton exchange from the bound $^{15}NH_4^+$ ions is not the major factor controlling the drop of autocorrelation peak volumes V_U and V_L at short mixing times. The initial steep decrease of V_U and V_L is characterized by rate constant B_1, which exhibits some temperature dependence in the 273−298 K range

(Table S1). The decrease of V_U and V_L at longer mixing times is characterized mainly by rate constant B_2. The temperature dependence of rate constants B_1 and B_2 corresponding to V_L is small, which is related to slow $^{15}NH_4^+$ ion movement from binding site L. On the other hand, the B_1 and B_2 rate constants corresponding to V_U exhibit a higher temperature dependence, which suggests more efficient $^{15}NH_4^+$ ion movement and relaxation processes. However, autocorrelation peak volumes V_L and V_U are influenced by a combination of several competing factors (including dipole−dipole-correlated relaxation) which have not been dissected.

The temperature dependence of rate constant k_{UB} has been used to calculate an activation energy of 66 kJ mol^{-1} for exchange of $^{15}NH_4^+$ ions from binding site U within $d(G_3T_4G_4)_2$ to the bulk solution. In comparison, the activation energy for exchange of Na^+ ions inside the $d(G_4T_4G_4)_2$ G-quadruplex is 22 kJ mol^{-1}.[36] The 3 times lower activation energy is in accordance with the smaller ionic radius of Na^+ ions, which can move more freely along the central axis of the G-quadruplex. The movement of bigger $^{15}NH_4^+$ ions requires partial opening of the G-quartets. We have shown previously that inner $^{15}NH_4^+$ ions move 7.5 times faster when a Na^+ ion is occupying the neighboring outer binding site of the $d(G_4T_4G_4)_2$ G-quadruplex.[32] However, the activation energy for cation movement depends on structural features of the individual G-quadruplex. The absence of cross-peaks for the movement between binding sites U and L within $d(G_3T_4G_4)_2$ suggests that the energy barrier for $^{15}NH_4^+$ ions to move is prohibitively high.

Our study demonstrates that cation movement through G-quadruplexes can be controlled by their inherent structural features. Apart from the first indication that G-quadruplexes with fold-back loops are not suitable candidates for ion channels, such knowledge is potentially useful in the design of synthetic ion channels where kinetics or gating of ion movement can be achieved through chemical modifications that influence the energy barriers for G-quartet opening.

Conclusions

In the present paper we describe a novel and unique observation of $^{15}NH_4^+$ ion movement within the G-quadruplex structure and with the bulk solution. NMR experiments have demonstrated that there is no exchange of $^{15}NH_4^+$ ions between binding sites U and L, and therefore, $d(G_3T_4G_4)_2$ does not resemble an ion channel. However, $^{15}NH_4^+$ ions move between the two binding sites and the bulk solution. The quantification of volume integrals of the UB and LB cross-peaks has shown that $^{15}NH_4^+$ ion movement into the bulk solution is 12 times more frequent from binding site U than from binding site L. The steric hindrance imposed by the diagonal-type loop compared to the edge-type loop requires significant conformational rearrangements for $^{15}NH_4^+$ ions to leave or enter the G-quadruplex core. Furthermore, the diagonal loop can induce a higher energy barrier for the partial opening of the outer G-quartet, which is required for $^{15}NH_4^+$ ions at binding site L to move through into the bulk. Our findings suggest that each G-quadruplex structure might have its own lowest energy pathway in which ions will move inside as well as exchange into the bulk solution. In principle, the $^{15}NH_4^+$ ion at each binding site within the G-quadruplex can move to one of the two neighboring binding sites or into the bulk solution in the case of the outer binding site. An understanding of the influence of different loop orientations on the rate of $^{15}NH_4^+$ ion movement is important to establish more general rules with the ultimate aim to predict which of the outer cation binding sites will exhibit faster ion movement. Our study represents a step toward the prediction of the preferred direction of $^{15}NH_4^+$ ion movement based on a 3D model of the G-quadruplex. Such knowledge is expected to guide future efforts to build synthetic ion channels based on G-quadruplex structures.

Acknowledgment. We thank the Slovenian Research Agency (ARRS) and the Ministry of Higher Education, Science and Technology of the Republic of Slovenia (Grant Nos. P1-0242-0104 and J1-6140-0104) for their financial support.

Supporting Information Available: Parameters from the curve fitting (Table S1) and volume integrals of the autocorrelation peaks in the 273−298 K range, Arrhenius plot, and regions of the ^1H NMR spectra at several concentrations of $^{15}NH_4^+$ ions (Figures S1−S5). This material is available free of charge via the Internet at http://pubs.acs.org.

JA0710003